Applied Surface Science 356 (2015) 1314–1319

Contents lists available at ScienceDirect

Applied Surface Science

journal homepage: www.elsevier.com/locate/apsusc

Top-down patterning and self-assembly of flower-like gold arrays for surface enhanced Raman spectroscopy

Zhezhe Wang[a,b], Zhuohong Feng[a,b], Lin Lin[a,b], Pingping Huang[a], Zhiqiang Zheng[a,b,*]

[a] College of Physics and Energy, Fujian Normal University, Fuzhou 350117, China
[b] Fujian Provincial Key Laboratory of Quantum Manipulation and New Energy Materials, Fuzhou 350117, China

ARTICLE INFO

Article history:
Received 11 June 2015
Received in revised form 24 August 2015
Accepted 27 August 2015
Available online 31 August 2015

Keywords:
Photosensitive sol–gel
Electrochemical reaction
Self-assembly
Flower-like gold arrays
SERS

ABSTRACT

A low-cost and controllable fabrication method of flower-like Au arrays has been developed by using photosensitive sol–gel and electrochemical reaction self-assembly strategy on a TiO_2 patterned Si substrate. The effects of concentration of $HAuCl_4$ solution and applied voltage have been investigated to tailor the growth of Au nanoflowers. At a proper applied voltage (12 V) and concentration (0.005 mM), fractal flower-like Au arrays is prepared and shows strong SERS effect. The concentration of detectable Rhodamine 6G can be down to 10^{-10} M using the short data integration time (5 s). These flower-like Au arrays with strong SERS effect could be used in biosensors and nanodevices with molecule-level detection.

1. Introduction

As a powerful and extremely sensitive spectroscopic technique, Surface-enhanced Raman Scattering (SERS) has attracted much attention in the past decade due to its wide applications in analytical chemistry, biomedical detection, and environmental monitoring [1–4]. For practical application, the ideal SERS substrates should have sufficiently high enhancement factors, and also be uniformity, reproducibility and facile synthesis. Noble metals such as gold (Au), silver (Ag) and copper (Cu) nanostructures should be the ideal SERS substrates for their localized surface plasmon resonance (LSPR), which show strong SERS enhancement [5–9]. In particular, due to the rapid development of micro or nano lithography, various ordered noble metallic arrays have be designed and engineered to work as the SERS substrates. Compared to smooth and random SERS substrates, these ordered metallic arrays could generate high electric field enhancement, and achieve broadband and unidirectional excitation of SPPs, even at normal incidence [10–12]. However, ordered metallic arrays based bottom-up approach face significant challenge of producing reproducible and uniform arrays [13], while, top-down approach such as electron or ion beam lithography could produce more uniform and reproducible nanostructures. But these techniques not only require time consuming serial processing in vacuum, but also are limited and very costly due to the requirements of specialized equipment with controlled environments [14,15]. Nanoimprint lithography could produce nanostructures with the advantages of lower cost, ease of use than the capital intensive equipment, however, still it may require the use of an elastomeric mold patterned with relief structures on its surface and after curing, the mold should be peeled away carefully [16,17].

In the work reported here, we combined top-down and bottom-up approaches, developing a low-cost and controllable method for flower-like Au arrays by means self-assembly and electrochemical reaction occurring inside the confined region by patterned organic–inorganic TiO_2 film microstructure on Si substrates. Specifically, the patterned TiO_2 microstructure was prepared by photosensitive sol–gel, which make the TiO_2 films with photosensitive properties through chelating the metal alkoxide titanium tetrabutoxide monomer ($Ti(O(CH_2)_3CH_3)_4$: Ti(O-n-Bu)$_4$) with the chemical modifier benzoylacetone ($C_6H_5COCH_2COCH_3$: BzAcH). The major advantage of this approach is that you can obtained inorganic or organic–inorganic composited materials microstructures even nanostructures with different sizes simply and rapidly by photo lithography but not using photoresist as sensitive medium [18–20]. At the same time, the flower-like Au arrays prepared by self-assembly and electrochemical reaction can grow tightly on the substrate and importantly show strong SERS effect. The details are reported in this paper.

* Corresponding author at: College of Physics and Energy, Fujian Normal University, Fuzhou 350117, Fujian, China.
E-mail address: zqzheng@fjnu.edu.cn (Z. Zheng).

http://dx.doi.org/10.1016/j.apsusc.2015.08.234
0169-4332/

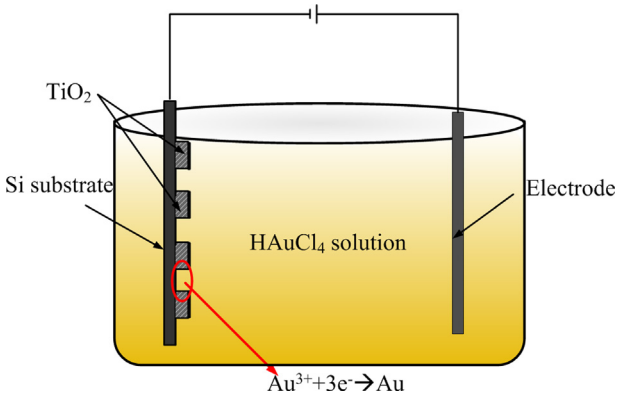

Fig. 1. Schematic illustration of the electrochemical system for fabricating the flower-like Au arrays.

2. Experimental

The TiO_2 photosensitive sol is synthesized by refluxing the Ti(O-n-Bu)$_4$ and BzAcH in the absolute methanol (CH_3OH:MeOH) with the molar ratio is 1:1:40 for 2–3 h. The homogeneous photosensitive TiO_2 gel films are prepared on Si substrates by dip-coating. And then, TiO_2 microstructure are fabricated by irradiating the gel film with UV light (Ushio SP-9 250DB, power 250W) through a mask followed by dissolving the non-irradiated area in a suitable solvent. After that, the microstructure should be heat-treated at 250 °C for 30 min to make it stable and reliable.

For a typical synthesis of flower-like Au arrays, the electrolyte containing $HAuCl_4$ solution is first prepared with distilled water. The patterned organic–inorganic TiO_2 microstructure on Si substrate is used as working electrode (or cathode), and a clean Zn sheet is used as auxiliary electrode (see Fig. 1). Because the organic–inorganic TiO_2 is insulated, the electrochemical reaction will occur mostly at the bare Si substrate. Thus, flower-like Au arrays can be generated. The effects of concentration of $HAuCl_4$ solution and applied voltage have been investigated to tailor the growth of Au nanoflowers. The sample is cleaned with distilled water for several times and dried before microstructural characterization and SERS measurement.

SERS measurements are carried out using a HORIBA Jobin Yvon LabRAM HR Evolution confocal microprobe Raman spectrometer with the 532 nm He–Ne Laser line at room temperature. Samples for SERS are dipped into the Rhodamine 6G (R6G) aqueous solution with concentrations of 10^{-5} M for 10 h, rinsed with de-ionized water, and dryed before measurement.

3. Results and discussion

Fig. 2 shows the SEM images of the as-prepared flower-like Au arrays on Si substrates. As shown in Fig. 2, the dark-colored part is TiO_2 film, while light-colored part is bare Si substrate. Owing to the electrical insulativity of organic–inorganic TiO_2, the electrochemical reaction occur only at the bared Si substrate, at where $[Au(OH)_4]^-$ has been reduced to flower-like Au(sold) [21]. Thus, an array of flower-like Au is generated on patterned Si substrate. The average diameter of each Au nanoflowers is about 60–120 nm.

Preferential growth of Au nanoflowers on TiO_2 patterned Si substrate has been investigated by changing the concentration of $HAuCl_4$ solution and applied voltage. Fig. 3 shows the SEM images of the Au nanoflowers on TiO_2 patterned Si substrate prepared with the applied voltage of 28 V (Fig. 3(a)), 24 V (Fig. 3(b)), 20 V (Fig. 3(c)), 16 V (Fig. 3(d)), 12 V (Fig. 3(e)), 8 V (Fig. 3(f)), 4 V (Fig. 3(g)) and 2 V (Fig. 3(h)), respectively. The experiments results show that: when the voltage is higher than 16 V, the isolated island Au nanostructure is formed on Si substrate. In contrast, reducing the applied voltage obviously facilitates the fractal growth of the Au nanoflowers, and meanwhile, the density of Au nanoflowers will be reduced. When the voltage is quite low (less than 2 V), the Au nanoflowers would not grow.

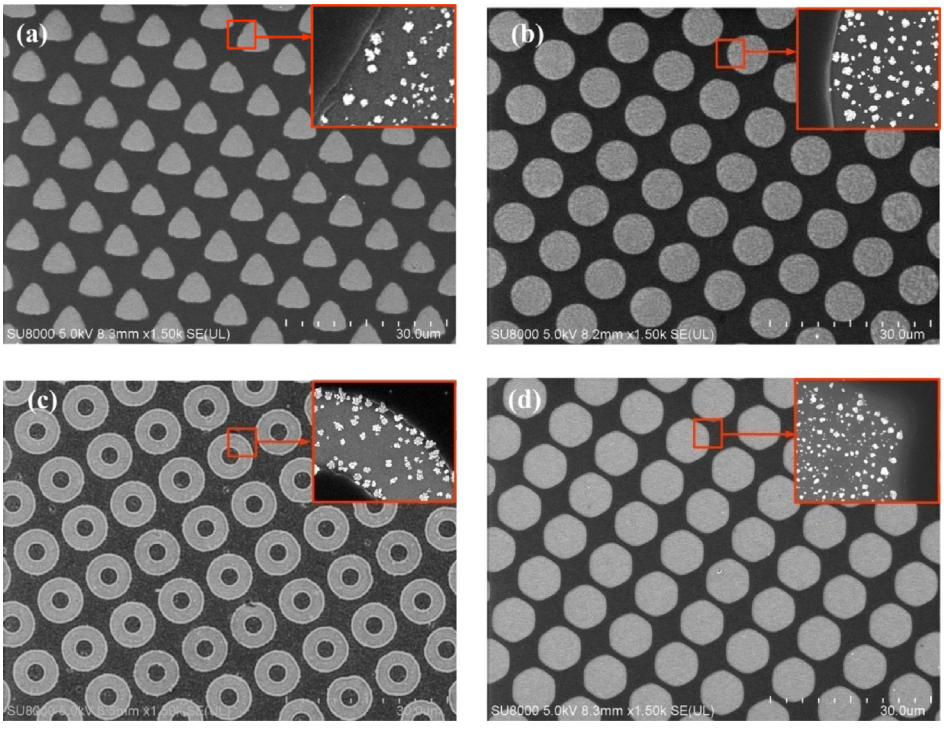

Fig. 2. SEM images of the as-prepared flower-like Au arrays using different TiO_2 microstructure on Si substrates. The concentration of $HAuCl_4$ solution is 0.005 mM.

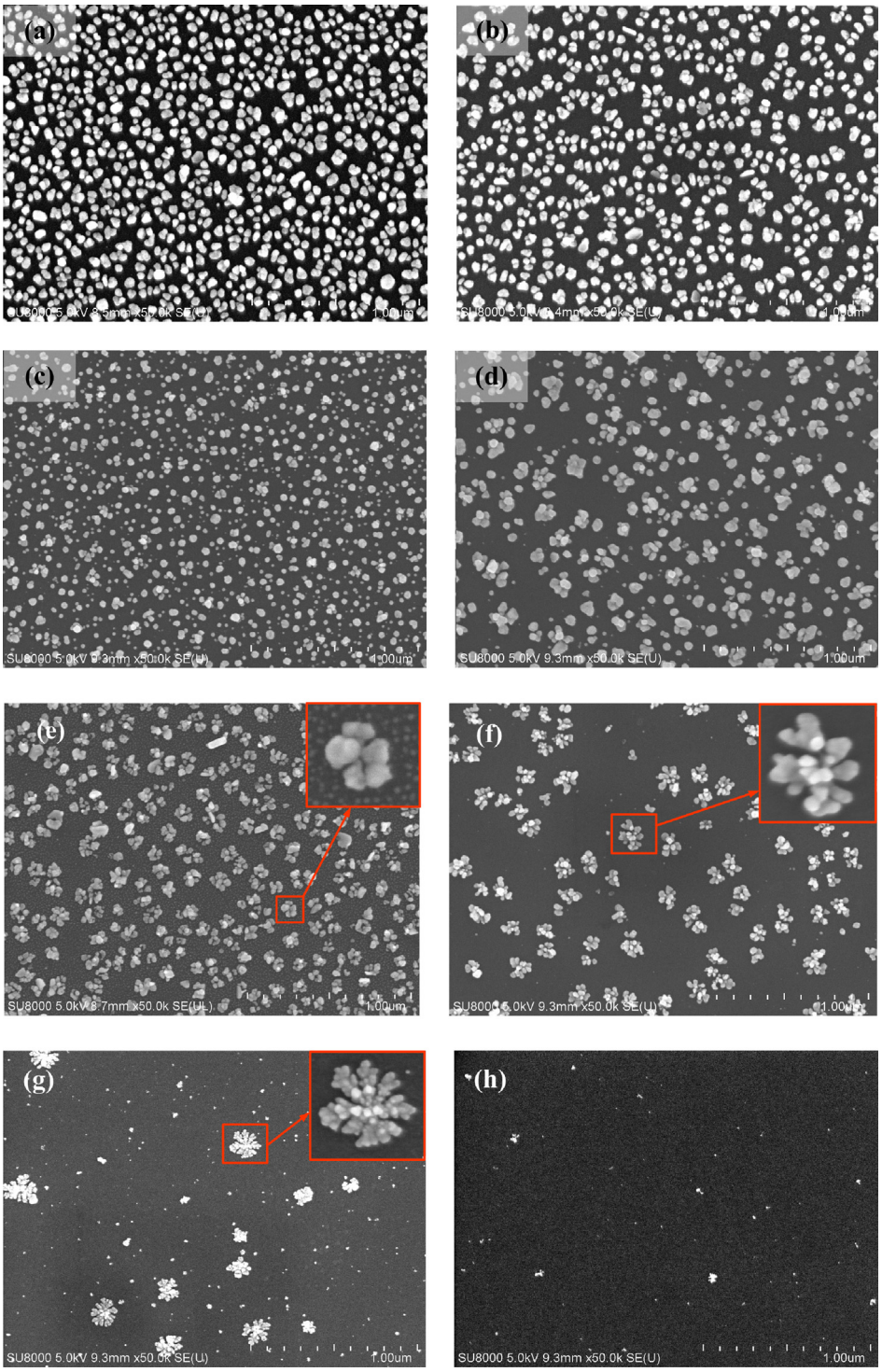

Fig. 3. SEM images of the Au nanoflowers on TiO_2 patterned Si substrate prepared with different applied voltage. The voltage of (a), (b), (c), (d), (e), (f), (g) and (h) is 28 V, 24 V, 20 V, 16 V, 12 V, 8 V, 4 V, 2 V, respectively. The concentration of $HAuCl_4$ solution is 0.005 mM and the deposition time is 40 min.

The concentration of $HAuCl_4$ solution has been played another important role in deciding which Au architecture is formed. Fig. 4 shows the SEM images of the Au nanoflowers on TiO_2 patterned Si substrate prepared with different concentration of $HAuCl_4$ solution. The concentration of (a), (b), (c) and (d) is 0.2 mM, 0.1 mM, 0.01 mM and 0.005 mM, respectively. From the experiment, we find that when concentration of $HAuCl_4$ solution is higher, isolated island or spherical Au nanostructure is formed as shown in Fig. 4(a)–(c). Decreasing concentration to 0.001 mM, very little Au can be deposited onto the Si substrate. Keeping the concentration of $HAuCl_4$ solution is 0.005 mM, fractal Au nanoflowers is easily obtained (see Fig. 4(d)).

On the basis of the previous discussion, the formation mechanism of Au nanoflowers can be illustrated by the schematic drawing in Fig. 5. Changing the concentration of $HAuCl_4$ solution and applied voltage gives one the ability to control the nucleation and growth processes through careful regulation of reaction rate. At elevated concentration or applied voltage, the

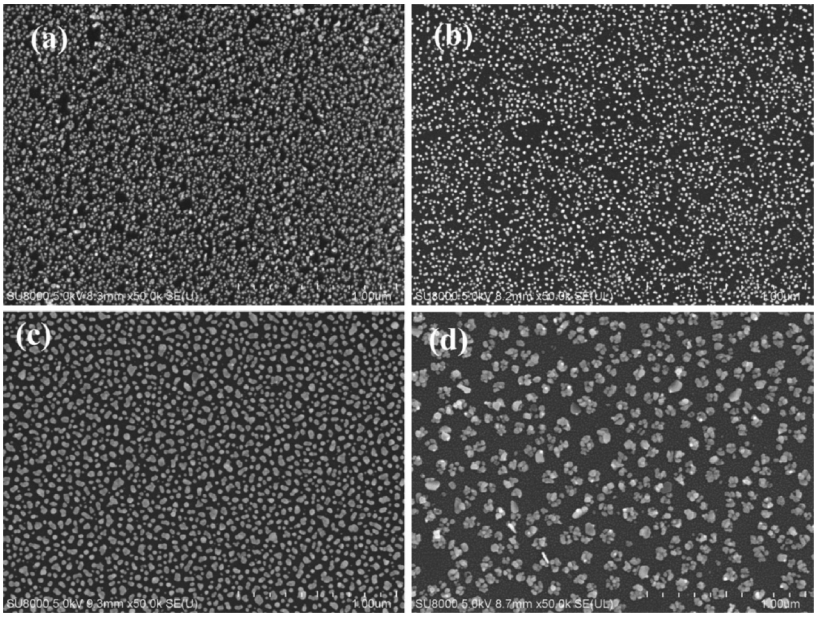

Fig. 4. SEM images of the Au nanoflowers on TiO_2 patterned Si substrate prepared with different concentration of $HAuCl_4$ solution. The concentration of (a), (b), (c) and (d) is 0.2 mM, 0.1 mM, 0.01 mM and 0.005 mM, respectively. The applied voltage is 12 V and the deposition time is 40 min.

reaction rate of Au^{3+} ions into Au atoms can be accelerated and thereby to accelerate the nucleation and isotropic growth steps (see Fig. 5(a)). The selected-area electron diffraction (SAED) pattern indicates that the spherical Au nanostructure exhibits single crystal structure. In contrast, lower concentration or applied voltage can reduce the reaction rate of Au^{3+} ions into Au atoms, which facilitates the anisotropic growth and formation of fractal Au nanoflowers (see Fig. 5(b)). The SAED pattern indicates

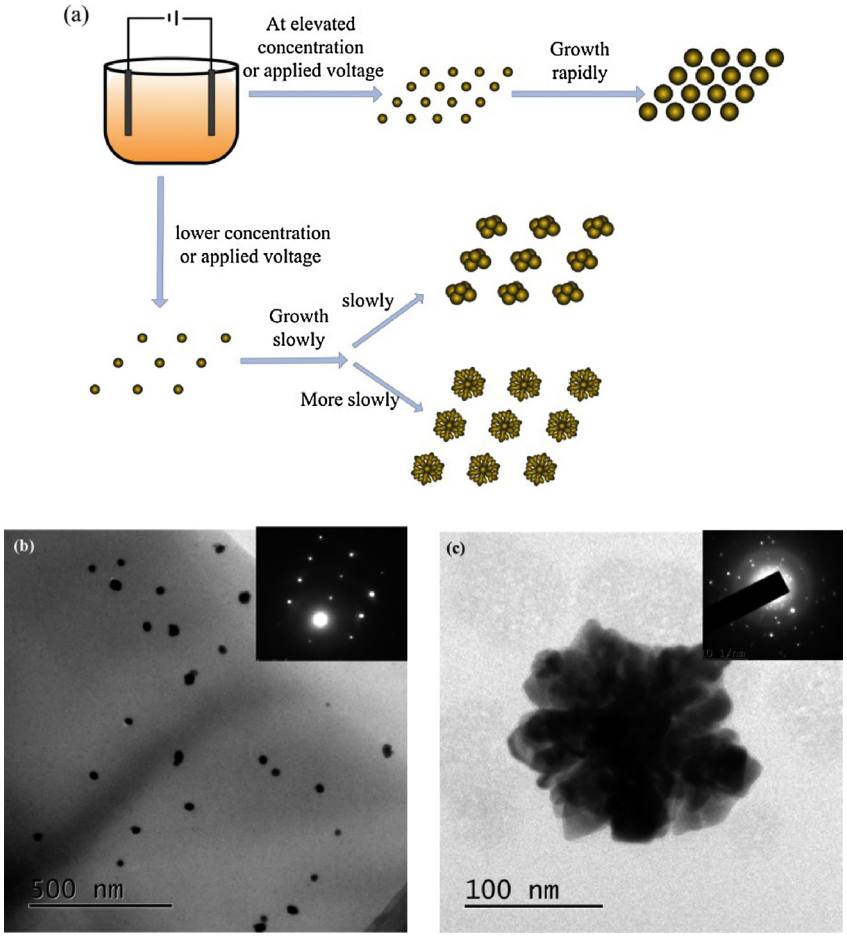

Fig. 5. Schematic drawing of the formation mechanism of Au nanoflowers. (b) and (c) is the TEM image of spherical Au nanostructure and fractal Au nanoflowers, respectively.

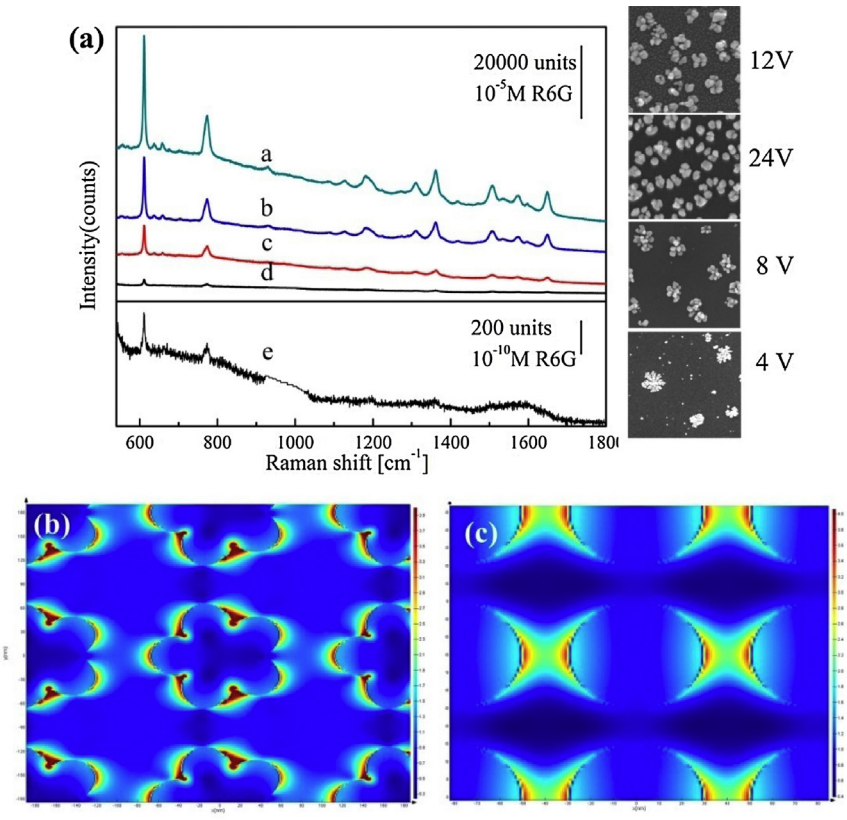

Fig. 6. SERS spectra for as-prepared flower-like Au array probed with (data integration time is 5 s). Curves a–d in (a) are SERS spectra probed with 10^{-5} M R6G corresponding to the Au arrays shown in Fig. 3(b), (a), (c) and (d). Curve e is SERS spectrum for flower-like Au array probed with 10^{-10} M R6G (data integration time: 5 s). (b) The spatial distribution of the electric field obtained by 3D FDTD simulation for flower-like Au array with the applied voltage of 12 V. (c) The spatial distribution of the electric field obtained by 3D FDTD simulation for spherical Au array with the applied voltage of 24 V.

that the structure of Au nanoflowers is polycrystalline, which can be ascribed to the random growth and aggregation model of the nanocrystals [22]. The detail growth mechanism of Au nanoflowers would be investigated and discussed in our further research.

The as-grown flower-like Au array show strong SERS effect by using R6G as probe molecules (see curves in Fig. 6(a) corresponding to different applied voltages). The SERS signal from Au nanoflowers is enhanced much more than from the isolated island Au nanostructure (see curves a and b of Fig. 6). In addition, from the curves c and d, it can be seen that the flower-like Au array with less Au nanoflowers (applied voltage: 8 V and 4 V) is of weaker SERS signal. Furthermore, in our experimental, the SERS signal has been obviously detected with 10^{-10} M R6G using the same data integration time (5 s) as seen in Fig. 6 curve e, which shows the possibility of molecule-level detection. The spatial distribution of electric field of Au array with the flower-like nanostructure and spherical nanostructure is studied by three dimensional finite-difference time-domain (3D FDTD) simulations (Lumerical FDTD Solution, Inc., Canada) to make a direct comparison with the experimental SERS results (see Fig. 6(b) and (c)) [23]. The total field/scattered-field plane wave source with the wavelength of 532 nm is selected and the polarization direction of is parallel to the horizontal direction. The mesh size of the override mesh region is set to be 1 nm. As shown in Fig. 6(b) and (c), the electromagnetic field (EM) enhancement in the gaps generated from Au array with the flower-like nanostructure is larger than the spherical-like nanostructure. These gaps are vital hot spots for SERS, which indicate that the enhancement factor of flower-like Au array is stronger than spherical-like Au array. The FDTD simulation results are consistent with the SERS spectra.

4. Conclusions

In summary, cost-effective SERS substrates with ordered Au arrays are successfully fabricated by means of photosensitive sol–gel and electrochemical reaction self-assembly on TiO_2 patterned silicon slides. The micro morphology of Au arrays can be controlled and tailored by modifying the concentration of electrolyte solution and applied voltage simply. In this study, fractal flower-like Au arrays prepared at the applied voltage of 12 V and concentration of 0.005 mM shows very strong SERS effect. The present investigation opens a possibility of applying such ordered fractal metallic arrays as SERS substrates offering excellent electric field enhancement and further interesting properties such as broadband and excitation of SPPs, which is of great importance for be used in biosensors and nanodevices with molecule-level detection.

Acknowledgements

The authors acknowledge the financial supports from the National Natural Science Foundation of China (Nos. 51202033 and 11204039), the Natural Science Foundation of Fujian Province of

China (No. 2015J01243) and the Science Foundation of the Educational Department of Fujian Province of China (No. JA13084).

References

[1] J. Li, Y. Huang, Y. Ding, Z. Yang, S. Li, X. Zhou, F. Fan, W. Zhang, Z. Zhou, D. Wu, B. Ren, Z. Wang, Z. Tian, Shell-isolated nanoparticle-enhanced Raman spectroscopy, Nature 464 (2010) 392–395.
[2] N. Savage, Trick of the light, Nature 495 (2013) s8–s9.
[3] S. Yang, X. Luo, Mesoporous nano/micro noble metal particles: synthesis and applications, Nanoscale 6 (2014) 4438–4457.
[4] K. Zhang, T. Zeng, X. Tan, W. Wu, Y. Tang, H. Zhang, A facile surface-enhanced Raman scattering (SERS) detection of rhodamine 6G and crystal violet using Au nanoparticle substrates, Appl. Surf. Sci. 347 (2015) 569–573.
[5] G. Duan, W. Cai, Y. Luo, Z. Li, Y. Li, Electrochemically induced flowerlike gold nanoarchitectures and their strong surface enhanced Raman scattering effect, Appl. Phys. Lett. 89 (2006) 211905–211911.
[6] A. Yang, J. Bi, S. Yang, J. Zhang, A. Chen, S. Liang, Highly surface-roughened caterpillar-like Au/Ag nanotubes for sensitive and reproducible substrates for surface enhanced Raman spectroscopy, RSC Adv. 4 (2014) 45856–45861.
[7] Q. Fu, D. Zhang, Y. Chen, X. Wang, L. Han, L. Zhu, P. Wang, H. Ming, Surface enhanced Raman scattering arising from plasmonic interaction between silver nano-cubes and a silver grating, Appl. Phys. Lett. 103 (2013) 041122–41131.
[8] J. Bian, S. Shu, J. Li, C. Huang, Y. Li, R. Zhang, Reproducible and recyclable SERS substrates: flower-like Ag structures with concave surfaces formed by electrodeposition, Appl. Surf. Sci. 333 (2015) 126–133.
[9] N. Dara, K. Chen, Y. Nien, N. Perkas, A. Gedankenc, I. Chen, Sonochemically synthesized Ag nanoparticles as a SERS active substrate and effect of surfactant, Appl. Surf. Sci. 331 (2015) 219–224.
[10] J.-S. Bouillard, S. Vilain, W. Dickson, G.A. Wurtz, A.V. Zayats, Broadband and broadangle SPP antennas based on plasmonic crystals with linear chirp, Sci. Rep. 2 (2012) 829.
[11] X. Li, H. Hu, D. Li, Z. Shen, Q. Xiong, S. Li, H. Fan, Ordered array of gold semishells on TiO_2 Spheres: an ultrasensitive and recyclable SERS substrate, ACS Appl. Mater. Interfaces 4 (2012) 2180–2185.
[12] C. Leordean, B. Marta, A. Gabudean, M. Focsan, I. Botiz, S. Astilean, Fabrication of highly active and cost effective SERS plasmonic substrates by electrophoretic deposition of gold nanoparticles on a DVD template, Appl. Surf. Sci. 349 (2015) 190–195.
[13] K. Jung, J. Hahn, S. In, Y. Bae, H. Lee, P.V. Pikhitsa, K. Ahn, K. Ha, J.K. Lee, N. Park, M. Choi, Hotspot-engineered 3D multipetal flower assemblies for Surface-Enhanced Raman Spectroscopy, Adv. Mater. 26 (2014) 5924–5929.
[14] K.R.V. Subramanian, M.S.M. Saifullah, E. Tapley, D.-J. Kang, M.E. Welland, M. Butler, Direct writing of ZrO_2 on a sub-10 nm scale using an electron beam, Nanotechnology 15 (2004) 158–162.
[15] K. Höflich, R. Yang, A. Berger, G. Leuchs, S. Christiansen, The direct writing of plasmonic gold nanostructures by electron-beam-induced deposition, Adv. Mater. 23 (2011) 2657–2661.
[16] P. Yang, T. Deng, D. Zhao, P. Feng, D. Pine, B.F. Chmelka, G.M. Whitesides, G.D. Stucky, Hierarchically ordered oxides, Science 282 (1998) 2244–2246.
[17] W. Zhang, F. Ding, W. Li, Y. Wang, J. Hu, S.Y. Chou, Giant and uniform fluorescence enhancement over large areas using plasmonic nanodots in 3D resonant cavity nanoantenna by nanoimprinting, Nanotechnology 23 (2012) 225301.
[18] Z. Wang, G. Zhao, W. Zhang, Z. Feng, L. Lin, Z. Zheng, Low-cost micro-lens arrays fabricated by photosensitive sol–gel and multi-beam laser interference, Photonics Nanostruct. 10 (2012) 667–673.
[19] Z. Wang, G. Zhao, L. Lin, Z. Feng, Z. Zheng, Fabrication of surface: relief gratings and their laser induced damage resistance properties, J. Sol-Gel Sci. Technol. 64 (2012) 480–484.
[20] G. Zhao, Z. Wang, G. Xu, X. Deng, Fabrication of PZT nano dot array and their ferroelectric properties, Microsyst. Technol. 18 (2012) 531–535.
[21] Y. Wu, K. Liu, B. Su, L. Jiang, Superhydrophobicity-mediated electrochemical reaction along the solid–liquid–gas triphase interface: edge-growth of gold architectures, Adv. Mater. 26 (2014) 1124–1128.
[22] J. Wang, X.-B. Zhang, Z.-L. Wang, L.-M. Wang, W. Xing, X. Liu, One-step and rapid synthesis of “clean” and monodisperse dendritic Pt nanoparticles and their high performance toward methanol oxidation and p-nitrophenol reduction, Nanoscale 4 (2012) 1549–1552.
[23] J. Lu, P. yang, X. Hu, Simulations of light scattering from a biconcave red blood cell using the finite-difference time-domain method, J. Biomed. Opt. 10 (2005) 024022.